One-Step Routes from Di- and Triblock Copolymer Precursors to Hydrophilic Nanoporous Poly(acrylic acid)-*b*-polystyrene

Fengxiao Guo,[†,‡] Katja Jankova,[‡] Lars Schulte,[†] Martin E. Vigild,*[,‡] and Sokol Ndoni*[,†]

Polymer Department, Risø National Laboratory, Technical University of Denmark, DK-4000 Roskilde, Denmark, and Danish Polymer Centre, Department of Chemical Engineering, NanoDTU, Technical University of Denmark, DK-2800 Kgs. Lyngby, Denmark

Received August 20, 2007; Revised Manuscript Received December 4, 2007

ABSTRACT: Nanoporous polystyrene with hydrophilic pores was prepared from di- and triblock copolymer precursors. The precursor material was either a poly(*tert*-butyl acrylate)-*b*-polystyrene (P*t*BA-*b*-PS) diblock copolymer synthesized by atom transfer radical polymerization (ATRP) or a polydimethylsiloxane-*b*-poly(*tert*-butyl acrylate)-*b*-polystyrene (PDMS-*b*-P*t*BA-*b*-PS) triblock copolymer synthesized by a combination of living anionic polymerization and ATRP. In the latter copolymer, PS was the matrix and mechanically stable component, P*t*BA was converted by acidic deprotection to hydrophilic poly(acrylic acid) (PAA) providing at the same time part of the nanoporosity, and PDMS was quantitatively etched to provide additional nanoporosity. Both the deprotection of the P*t*BA block and the etching of PDMS were realized by one-step operations using either anhydrous hydrogen fluoride (HF) or trifluoroacetic acid (TFA). The finding that TFA can remove PDMS is important, not least as an alternative to the more hazardous HF. The investigated di- and triblock copolymer samples were of either hexagonal or lamellar morphology. The resulting nanoporous polymers were characterized by infrared spectroscopy, small-angle X-ray scattering, and scanning electron microscopy. In contact with water, all the prepared nanoporous polymers showed spontaneous water uptake close to the amounts expected from the precursor block copolymer compositions.

Introduction

The self-organization of block copolymers has attracted considerable attention in relation to "bottom up" nanotechnology because it enables various highly ordered structures at nanometer length scale. Specific removal of a minority component from an ordered block copolymer allows for the preparation of nanoporous materials. Nanoporous polymeric materials derived from self-organized block copolymers show great potential for nanoobject templates,[1−5] separation membranes,[6] sensors,[7,8] substrates for catalysis,[9] and hydrogen storage systems.[10] The exciting development of the field of nanoporous polymeric materials was recently reviewed by Hillmyer.[11]

Since the first nanoporous material preparation from an ordered block copolymer by Lee et al. in 1988,[12] a number of nanoporous polymers with hydrophobic cavities have been described. However, many possible applications such as drug delivery, growth of bacteria, and selective separation will require the nanoporous polymers to work in an aqueous environment. Only a limited number of nanoporous polymers with hydrophilic pores have been prepared to date. Liu and co-workers reported the preparation of nanoporous films from poly(2-cinnamoylethyl methacrylate)-*b*-poly(*tert*-butyl acrylate) (PCEMA-*b*-P*t*BA) and polyisoprene-*b*-poly(2-cinnamoylethyl methacrylate)-*b*-poly(*tert*-butyl acrylate) (PI-*b*-PCEMA-*b*-P*t*BA)/P*t*BA polymer blend. In both cases PCEMA was cross-linked by UV irradiation. The P*t*BA homopolymer was extracted in dichloromethane, and the *tert*-butyl groups in the copolymer were hydrolyzed in a dichloromethane solution of trimethylsilyl iodide followed by a methanol/water solution either in a two-pot or a one-pot procedure.[13,14] Hillmyer and co-workers prepared nanoporous polystyrene-*b*-poly(ethylene oxide) (PS-*b*-PEO) by treating PS-*b*-PEO/polystyrene-*b*-polylactide (PS-*b*-PLA) polymer blends in a sodium hydroxide water/methanol solution, which lead to cleavage of the PLA component.[15] The preparation of nanoporous polystyrene-*b*-poly(*N*,*N*-dimethylacrylamide) (PS-*b*-PDMA) by etching PLA block from PS-*b*-PDMA-*b*-PLA triblock copolymer was also reported by the same group.[16]

In this report, we present two new routes for generating hydrophilic nanoporous polymers; the first route uses hydrogen fluoride (HF) and the second one trifluoroacetic acid (TFA). The block copolymer precursors are either diblock copolymers of polystyrene and poly(*tert*-butyl acrylate) (PS-*b*-P*t*BA) or triblock copolymers of PS, P*t*BA, and polydimethylsiloxane (PS-*b*-P*t*BA-*b*-PDMS) prepared by combined atomic transfer radical and living anionic polymerizations.[17,18] The treatment of each of these polymers with either HF or TFA in one step invariantly resulted in nanoporous PS-*b*-PAA with hydrophilic cavities of poly(acrylic acid) (PAA). To the best of our knowledge, this is the first report on the preparation of such a hydrophilic nanoporous polymer. From the chemical point of view, it is not a surprise that the strong acid HF both deprotects the *tert*-butyl ester groups and degrades PDMS, leaving structurally and chemically intact the PS matrix. The real surprise is that the much weaker acid (and much less hazardous!), TFA, could also do the job; both deprotect *tert*-butyl esters (known) and remove PDMS (unknown), conserving the structure of the PS matrix. The finding that a chemical compound like TFA can remove PDMS is important, not least as an alternative to the more hazardous HF. The chemical synthesis procedure to prepare PDMS-*b*-P*t*BA-*b*-PS triblock copolymer precursors is also reported here.

Experimental Section

Materials. Tetrahydrofuran (THF) (Merck, ≥99%, stabilized with 0.025% butylated hydroxytoluene) was passed through a

* Corresponding authors. E-mail: mev@kt.dtu.dk; sokol.ndoni@risoe.dk.
† Polymer Department, Risø National Laboratory.
‡ Danish Polymer Centre, Department of Chemical Engineering, NanoDTU.

10.1021/ma0718806 CCC: $40.75
Published on Web 01/23/2008

column of active aluminum oxide and then was refluxed over sodium in the presence of benzophenone until a deep purple color was attained. The building block of PDMS (hexamethylcyclotrisiloxane or D_3) (Aldrich, 98%) was stirred over calcium hydride (CaH_2) for 4 h at 65 °C and distilled into a flask containing vacuum-dried dibutylmagnesium. After stirring for another 4 h, D_3 was distilled off again in an ampule just before use. The two monomers *tert*-butyl acrylate (*t*BA) (Fluka, ≥98%) and styrene (St) (Aldrich, 99%) were passed through a column of active aluminum oxide. The monomers as well as *m*-xylene (Aldrich, 99+%) or triethylamine (TEA) were then stirred over CaH_2 for 4 h at room temperature and distilled before use. Anhydrous HF (Holz+Co, Germany) and TFA (Aldrich, 98%) were used as received as degradation reactants. All other chemicals were received from commercial sources and used without further pretreatment.

Synthesis of P*t*BA-*b*-PS Diblock Copolymers by ATRP. The polymerizations were performed in argon as previously described.[19] *t*BA was polymerized with 2-EBP as the initiator at 60 °C. After purification the homopolymers were further employed as macroinitiators for a second ATRP of styrene in xylene at 100 °C.

Synthesis of PDMS-*b*-P*t*BA-*b*-PS Triblock Copolymer by a Combination of Anionic Polymerization and ATRP. *PDMS−H by Anionic Polymerization*. The polymerization was performed using an inert atmosphere system.[20] 700 mL of purified THF was distilled into the reactor. 2.6 mL of *sec*-butyllithium was added to the system using a syringe, and upon the addition of initiator the color of the solution became yellowish. The reactor was cooled to −5 °C in an isopropanol/dry ice bath. Then 12.4 g of D_3 was introduced as a 20 wt % THF solution into the reactor, and the color disappeared immediately, indicating that the polymerization started. After 3 days at 0 °C, the polymer was terminated with 1.3 mL of chlorodimethylsilane. The homopolymer (PDMS−H) was precipitated using methanol and dried in vacuum.

PDMS−Br Macroinitiator. Hydroxyl-terminated PDMS was first prepared: 8 mL of toluene, 0.41 mL of allyl alcohol, and 0.016 mL of Pt catalyst were charged into a reactor with stirring. The reactor was heated to 50 °C in an oil bath. Then 8 g of PDMS−H was introduced into the reactor dropwise by a syringe, and the temperature was raised to 65 °C for 2 h. Toluene and excess allyl alcohol were removed under vacuum at 100 °C. After cooling to room temperature, the resultant mixture was diluted with THF, and the product PDMS−OH was precipitated in methanol and dried in vacuum. The synthesis of PDMS−Br was then performed. 0.047 g of DMAP and 50 mL of dry THF were charged into a two-necked round-bottom flask equipped with a stirrer bar, condenser, and a dripping funnel, and 0.14 mL of dry TEA was added under nitrogen through the septum of the dripping funnel with a long needle. The flask was cooled to 0 °C in an ice bath. 0.071 mL *a*-bromoisobutyryl bromide was injected into the flask by a gas tight syringe. Then 6.61 g of PDMS−OH in 50 mL dry THF was transferred to the dripping funnel and slowly added to the flask under stirring for 1 h. The temperature was allowed to rise to room temperature. The mixture was stirred overnight, and then the THF was evaporated. The crude product was dissolved in 100 mL of CH_2Cl_2 and purified by washing several times with water (5 wt % aqueous $NaHCO_3$) and water again. The solution was dried overnight with $MgSO_4$ and filtered, and the CH_2Cl_2 was evaporated. A slightly yellow liquid product (PDMS−Br) was obtained, which was dried in vacuum.

PDMS-b-PtBA-b-PS Triblock Copolymer. The diblock copolymer of PDMS and P*t*BA was synthesized in bulk at 60 °C for 3.5 h using PDMS−Br as macroinitiator. The diblock copolymer macroinitiator PDMS-*b*-P*t*BA-Br was further utilized in an ATRP of styrene in xylene at 100 °C to give the triblock copolymer.

Annealing. P*t*BA-*b*-PS diblock and PDMS-*b*-P*t*BA-*b*-PS triblock copolymers were dissolved in THF, and the solutions were poured into Petri dishes. The solutions were left for 3 days to evaporate slowly under a slight flow of argon at room temperature. The solvent-cast samples were annealed in a homemade gastight steel cylinder under argon at 130 °C for 5 days and then gradually cooled down to room temperature.

Deprotection of P*t*BA and Etching of PDMS. *With HF*. The deprotection of P*t*BA and etching of PDMS with anhydrous HF were accomplished using standard HF equipment for cleaving synthetic peptide resins[21] at 0 °C for 2 h. The detailed procedure is the same as the one described in ref 22.

With TFA. The PDMS-*b*-P*t*BA-*b*-PS triblock copolymer film was stirred for 3 h in large molar excess of TFA relative to PDMS repeating unit. Afterward, the sample was washed in methanol for 24 h before drying under an argon stream at room temperature.

Characterization Methods. Size exclusion chromatography (SEC) experiments were performed at room temperature with two mixed-D columns from Polymer Laboratories. Stabilized THF was used as a solvent with a flow rate of 1 mL/min. The calibration line was constructed from SEC data of PS narrow molecular weight standards in the range $7 \times 10^2 - 4 \times 10^5$ g/mol. Molecular weight distributions relative to PS calibration were determined by processing the differential refractive index signal from a Viscotek model 200 detector. ^{1}H NMR spectra were recorded in $CDCl_3$ on a 250 MHz Avance DPX 250 Bruker instrument. FT-IR spectra were measured on a Perkin-Elmer SpectrumOne FT-IR spectrometer. Small-angle X-ray scattering (SAXS) patterns were acquired at the Risø National Laboratory using Cu Kα X-rays with a wavelength of $\lambda = 1.54$ Å. Scanning electron microscopy (SEM) measurements were done on a Zeiss 1540 EsB Gemini instrument at the Center for Microtechnology and Surface Analysis at the Danish Technological Institute. The samples for SEM were prepared by freeze fracturing in liquid nitrogen. 2−3 nm gold layer was sputtered onto the samples prior to imaging. Water uptake experiments were carried out by placing dry samples in glass vials containing water and kept under gentle stirring at room temperature. After being submerged for a certain time, a fine tissue was used to dry the surfaces of the sample quickly before weighing.

Results and Discussion

Synthesis of P*t*BA-*b*-PS Diblock Copolymer. The synthesis of P*t*BA-*b*-PS diblock copolymers was accomplished by ATRP of each of the monomers in the given order. Here we present results on two P*t*BA-*b*-PS diblock copolymers: AS-1 and AS-3. AS-1 has a number-average molecular weight M_n of 14.5 kg/mol, a polydispersity index (PDI) of 1.17, and mass fraction of P*t*BA of 0.54. AS-3 has a number-average molecular weight M_n of 25.0 kg/mol, a PDI of 1.20, and mass fraction of P*t*BA of 0.31.

Synthesis of PDMS-*b*-P*t*BA-*b*-PS Triblock Copolymer. PDMS-*b*-P*t*BA-*b*-PS triblock copolymer was synthesized by a combination of living anionic polymerization and ATRP according to Scheme 1.

PDMS macroinitiators for ATRP have previously been prepared by anionic polymerization.[23−25] Here we have chosen to use a modified three-step procedure, where the product of living anionic polymerization of D_3 was end-capped with chlorodimethylsilane, as shown in reaction step ii of Scheme 1. The yielded PDMS−H was coupled with allyl alcohol in the presence of Karstedt's catalyst[26] (see reaction step iii in Scheme 1) producing PDMS with a hydroxyl end group (PDMS−OH). Further reaction with α-bromoisobutyryl bromide[27] turned the obtained PDMS−OH into a bromoisobutyrate PDMS (PDMS−Br), shown in reaction step iv. PDMS−Br's role as a macroinitiator for ATRP is well documented.[23−25,27] The complete conversion of the mentioned groups in the functional PDMS through each of the steps was evidenced by ^{1}H NMR, as shown in Figure 1. The characteristic Si−H proton peaks in the hydrosilyl end group of PDMS−H at 4.7 ppm were found to disappear, and a new resonance with the double relative intensity at 3.6 ppm appeared, corresponding to the CH_2 adjacent to the hydroxyl unit in PDMS−OH. Furthermore, the signals for the CH_2 with the same relative intensity were shifted from 3.6 to

Scheme 1. Synthesis of PDMS-*b*-P*t*BA-*b*-PS Triblock Copolymer by a Combination of Living Anionic Polymerization and ATRP (Chemical Structure of the Final Triblock Copolymer Is Shown in the Last Row)

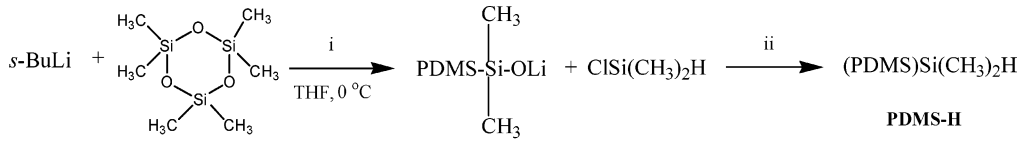

(Living anionic polymerization)

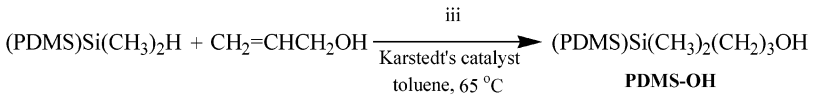

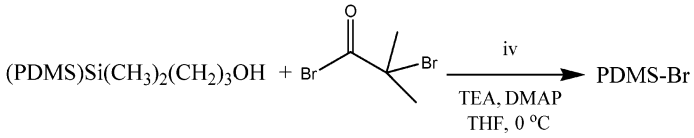

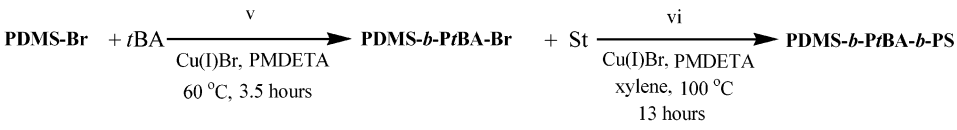

(ATRP)

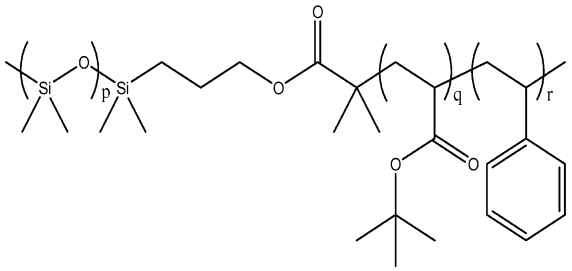

4.1 ppm as a result of replacing hydroxyl group by α-bromoisobutyryloxy group in the preparation of the macroinitiator. This is an indication of a virtually quantitative Si−H end group conversion to a brominated end group. As a direct check, the areas under the peaks a and d in the bottom panel of Figure 1 have the same value within the measurement accuracy. The group of peaks a represents the six methyl protons of the initiator and the peak d the six methyl protons of the Br-containing end group. In the top two spectra of Figure 1 the peaks at 3.7 and 1.8 ppm are from traces of THF in the polymer, and peaks around 3.5 and 1.6 ppm are caused by impurity of methanol and H_2O, respectively.

The obtained PDMS−Br was used to consecutively polymerize *t*BA and St blocks by ATRP. The size exclusion chromatography traces illustrating increased molecular weight from the macroinitiator (trace a) to the diblock (trace b) and finally to the triblock (trace c) are shown in Figure 2. The final PDMS-*b*-P*t*BA-*b*-PS triblock copolymer (DAS-1) has a number-average molecular weight M_n of 59.5 kg/mol and mass fractions of PDMS, P*t*BA, and PS of 0.17, 0.16, and 0.67, respectively, as determined by ^{1}H NMR. A polydispersity index (PDI) of 1.29 relative to PS calibration was estimated by SEC.

The data on the molecular weight, molecular weight distribution, and composition for the two P*t*BA-*b*-PS diblocks and the one PDMS-*b*-P*t*BA-*b*-PS triblock are summarized in columns 2−6 of Table 1. The compositional and mass dispersion are higher for these samples as compared to, e.g., block copolymers prepared by living anionic polymerization.[20,22,28] This increased dispersion correlates to lowered structure regularity, as will be seen in the following.

Small-angle X-ray scattering (SAXS) analysis of the annealed diblock and triblock copolymer samples revealed lamellar structure with average period of 25 nm in AS-1 and hexagonally packed cylindrical structure with respective principal spacings of 27 and 47 nm in AS-3 and DAS-1. The structure and the characteristic spacings of the three block copolymers, as determined by SAXS, are shown in the last two columns of Table 1. The organization of PDMS and P*t*BA within the cylindrical domains of DAS-1 is assumed to be of core−shell type with PDMS occupying the core.

Deprotection and Etching. The use of HF as a PDMS degrading agent in block copolymers was first reported 4 years ago.[22] HF quantitatively cleaves the Si−O bonds transforming them into Si−F bonds and was used to create nanoporous PS and polydiene materials.[22,29] Anhydrous HF is a strong protonating acid.[30] Our idea was to prepare a hydrophilic nanoporous material from a P*t*BA-*b*-PS diblock copolymer simply by deprotecting the P*t*BA block (i.e., creating PAA by cleaving the *tert*-butyl group). Obviously, the deprotection of P*t*BA should happen as a heterogeneous reaction in conditions of solid state (nonsolvent) for PS. HF successfully deprotected P*t*BA in both the P*t*BA-*b*-PS diblock and the PDMS-*b*-P*t*BA-*b*-PS

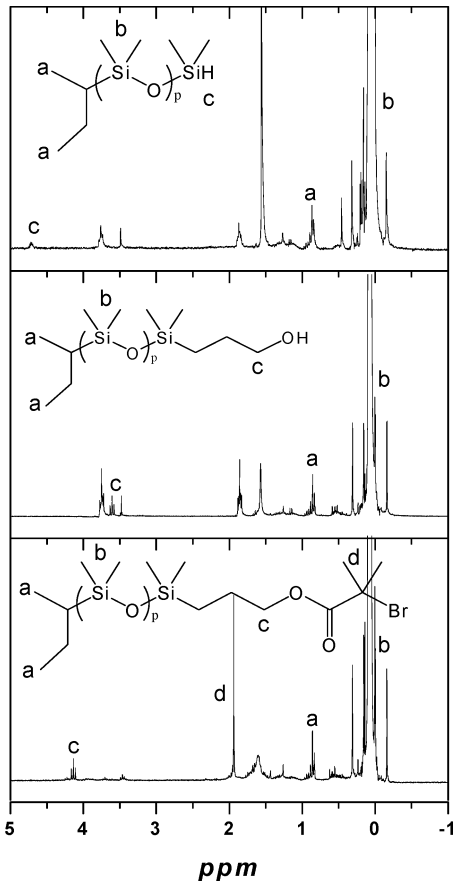

Figure 1. ^{1}H NMR spectra of PDMS−H (top), PDMS−OH (middle), and PDMS−Br (bottom).

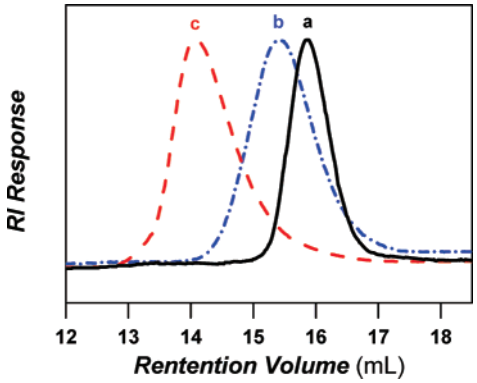

Figure 2. SEC monitoring the synthesis of triblock copolymer. (a) PDMS−Br (PDI = 1.08), (b) PDMS-*b*-P*t*BA (PDI = 1.20), (c) PDMS-*b*-P*t*BA-*b*-PS (PDI = 1.29).

Table 1. Molecular and Bulk Morphological Characteristics of the P*t*BA-*b*-PS and PDMS-*b*-P*t*BA-*b*-PS Samples

sample	M_n(NMR) (g/mol)	PDI (SEC)	w_{PS}	w_{PtBA}	w_{PDMS}	morphology[a] (SAXS)	d_{SAXS}[b] (nm)
AS-1	14 500	1.17	0.46	0.54		LAM	25
AS-3	25 000	1.20	0.69	0.31		HEX	27
DAS-1	59 500	1.29	0.67	0.16	0.17	HEX	47

[a] LAM = lamellar, HEX = hexagonally packed cylindrical structure. [b] Principal spacings d_{10} or lamellar spacing period d from SAXS.

triblock. Furthermore, the HF treatment also caused the already established degradation of PDMS in the case of the triblock copolymer. The deprotection reaction mechanism of P*t*BA by HF is expected to be a typical acidic deprotection for the case, involving a *tert*-butyl cationic intermediate and the final production of isobutylene.[31] *tert*-Butyl alcohol is also a possible

Scheme 2. Deprotection and Etching of Diblock P*t*BA-*b*-PS or Triblock PDMS-*b*-P*t*BA-*b*-PS Copolymers (by HF or TFA) Creates Nanoporous PAA-*b*-PS

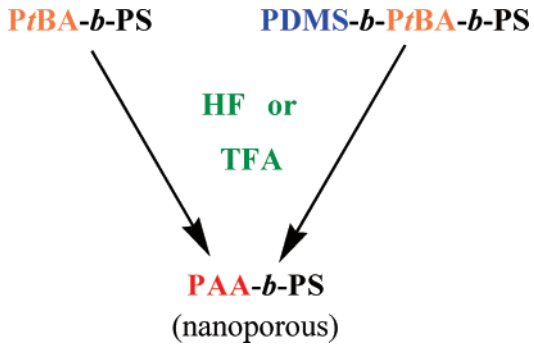

byproduct in the presence of water liberated by the cleavage of the Si−O bonds.[22] Treatment by excess HF constitutes the first one-step route of fabrication of hydrophilic nanoporous PAA-*b*-PS.

The use of HF is hazardous and should only be undertaken following strict safety precautions.[22] A known route for acidic deprotection of P*t*BA[31] is the use of anhydrous TFA in dichloromethane[32] or concentrated hydrochloric acid in dioxane.[33,34] The tentative treatment of the PDMS-*b*-P*t*BA-*b*-PS triblock copolymer with pure TFA (without any solvent) turned out to deprotect P*t*BA and simultaneously remove PDMS. The first interpretation of these results evokes acydolysis by TFA of all the ester bonds in the triblock copolymer, including the chain−backbone ester bond connecting PDMS with PtBA (see the last line in Scheme 1). Yet, this ester bond is expected to be stable to TFA; therefore, at present we do not have a good explanation for the surprising quantitative removal of the PDMS block by TFA. Furthermore, and most surprisingly, we have experienced that TFA actually removes PDMS even from anionically prepared PS−PDMS and polybutadiene−PDMS block copolymers (data not shown), where the transition bond from the hydrocarbon to the PDMS block is expected to be a carbon−silicone bond.[22,28] Treatment by excess TFA constitutes the second one-step route of fabrication of hydrophilic nanoporous PAA-*b*-PS.

Two instances were traced in the literature, reporting the combined use of TFA and PDMS. First, TFA has been described as a catalyst in cationic polymerization of cyclosiloxanes.[35,36] Second, DeSimone et al. used TFA with supercritical carbon dioxide to remove PDMS from a PS-*b*-PDMS block copolymer, which was prepared with a "weak" carbon−oxygen−silicone link between the blocks. The TFA was attributed to be able to cleave this link and the following treatment removed the PDMS.[37]

Our preliminary results hint to the use of TFA as a general PDMS-cleaving agent in block copolymers. The detailed study of the reaction between TFA and PDMS is in progress and will be reported elsewhere. Our findings on the creation of hydrophilic nanoporous polymers are summarized in Scheme 2.

Within 1−5% the mass loss after acidolysis, as measured by the ratio $\Delta m/\Delta m_{max}$ between the observed mass loss and the maximal expected value, was consistent with either the fraction of *tert*-butyl groups for diblock copolymer precursors (AS-1 and AS-3) or the fraction of its sum with the PDMS block for the triblock copolymer precursor (DAS-1).

Detailed information on the chemical composition changes for DAS-1 after HF and TFA treatments was acquired by the FT-IR spectra shown in Figure 3. Only the absorbance range of interest is presented in the figure. The spectrum of PDMS-

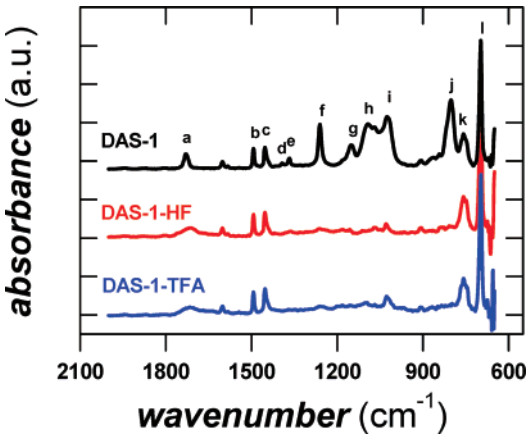

Figure 3. FT-IR spectra of DAS-1 precursor sample (top line), after HF treatment (middle line) or after TFA treatment (bottom line). Peaks are identified as follows: (a) C═O stretching (1730 cm^{-1}) in ester group, (b and c) CH stretching (1489, 1454 cm^{-1}) in monosubstituted phenyl group, (d and e) CH_3 bending (1394, 1368 cm^{-1}) in *t*Bu group, (f) CH_3 bending (1261 cm^{-1}) in Si−CH_3 and C−C−O stretching (1259 cm^{-1}) in O-*t*Bu, (g) C−O stretching (1151 cm^{-1}) in O-*t*Bu, (h and i) Si−O−Si stretching (1088−1092 cm^{-1}), (j) C−Si−C stretching (800 cm^{-1}) and (k and l) monosubstituted phenyl group (760, 700 cm^{-1}).

b-P*t*BA-*b*-PS (DAS-1) shows absorption bands related to the PDMS: CH_3 bending, Si−O−Si stretching, and C−Si−C stretching peaks located at 1261, 1092−1088, and 800 cm^{-1}, respectively. C═O (ester) stretching peak at 1730 cm^{-1}, CH_3 (*t*Bu) bending peak at 1394/1368 cm^{-1}, C−C−O stretching (O-*t*Bu) at 1259 cm^{-1}, and C−O (O-*t*Bu) stretching peak at 1151 cm^{-1} represent *tert*-butyl group in P*t*BA. The characteristic absorption peaks associated with PS are at 1489, 1454, 760, and 700 cm^{-1}. After deprotection and etching in HF for 2 h (DAS-1-HF), the characteristic peaks for PS remained intact, while the peaks related to PDMS (CH_3 bending and C−O stretching) and peaks originating from *tert*-butyl group disappeared entirely. The sharp peak (a in Figure 3) corresponding to the ester carbonyl group (C═O) was broadened after HF treatment due to the formation of carboxylic acid carbonyl group. The spectrum confirms that PDMS and *tert*-butyl groups were completely removed and PS was stable under HF treatment conditions. This shows that HF was also able to deprotect P*t*BA (yielding the hydrophilic PAA block) in addition to etching of PDMS. Identical chemical composition changes follow from TFA treatment (DAS-1-TFA) as shown in Figure 3.

Figure 4 shows SAXS 1D profiles of AS-1, AS-3, and DAS-1 before and after degradation. DAS-1 was treated with TFA and HF, and both curves are shown in panel c of Figure 4. The ratios of scattering peak positions for the HF-treated samples were identical to those for the original diblock and triblock precursors. But the scattering intensity was significantly increased after HF or TFA treatment for all three samples, though at different degrees. This is due to an increased electron density contrast as a result of replacing the removed chain parts by vacuum. The SAXS data give evidence for the creation of nanoporous structures of the same morphologies as that of the respective diblock and triblock precursors. We will discuss the nanoporous structures in more detail in the following section.

Nanoporous Structures. The positions of the primary peak q^* for AS-3-HF, DAS-1-HF, and DAS-1-TFA after HF treatment or TFA treatment matches the positions of the primary peak before etching, as can be seen from Figure 4b,c. These three samples all have cylindrical hexagonal morphology, which is invariant to the deprotecting procedure because of the glassy state of the matrix formed by the majority block (PS). However,

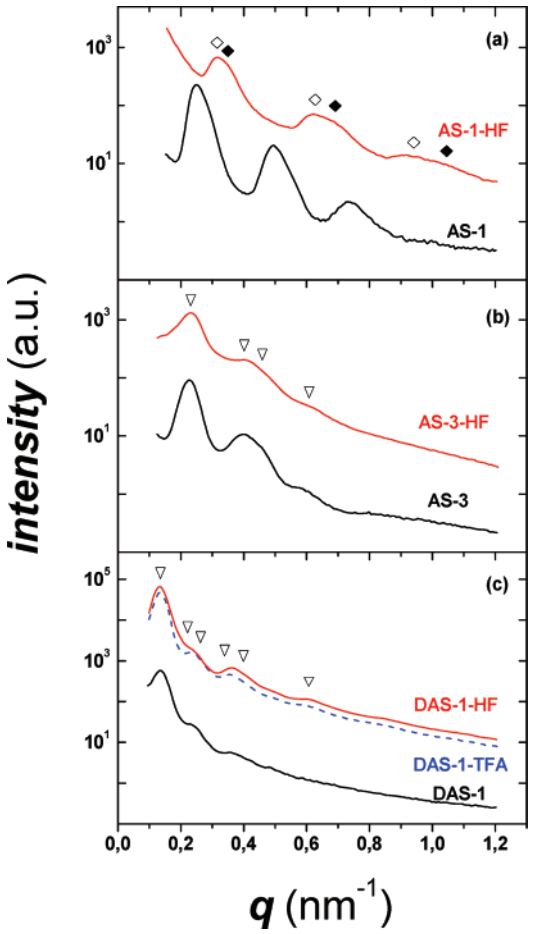

Figure 4. SAXS 1D profiles of (a) AS-1, (b) AS-3, and (c) DAS-1 before and after degradation. In panel a the expected reflections for a lamellar morphology are marked by diamonds (1:2:3), and in panels b and c some of the expected reflections for a hexagonally cylindrical morphology are marked by triangles ($1:3^{1/2}:4^{1/2}:7^{1/2}:9^{1/2}:21^{1/2}$). The filled diamonds in panel a mark the calculated *q*-scale for collapsed lamellae (see first paragraph of the Nanoporous Structures section and the Supporting Information[38]).

Figure 5. Schematic illustration of lamellar structure in AS-1 before and after deprotection: black, PS; orange, P*t*BA; red, PAA. PS is thought to remain unchanged during HF treatment. The P*t*BA (orange in the left panel) loses 44% by mass during HF acydolysis, converting into PAA (red in the right panel). The generated free volume gives rise to interlamellar nanocavities in the dry state, but the lamella packing gains disorder as schematized in the right panel and discussed in the text.[38]

for the lamellar sample AS-1-HF the peak position is not invariant to the deprotection of the minority block. The position of the primary peak for AS-1-HF increased from 0.253 to 0.321 nm^{-1} as can be seen in Figure 4a. This peak shift indicates that there was shrinkage of AS-1-HF during the degradation procedure. According to the incoherent scattering (at high *q*), the scattering contrast between AS-1-HF and AS-3-HF compared to their precursors are in the same order of magnitude, so we assume that both the etched samples have similar electron density profile although they are not of similar morphologies. The scattering peaks of AS-1-HF became broader and asymmetrical, which indicates that the lamellar morphology in the nanoporous AS-1-HF is not as well-defined as in the AS-1 precursor. This might be because there is no physical stabilizing

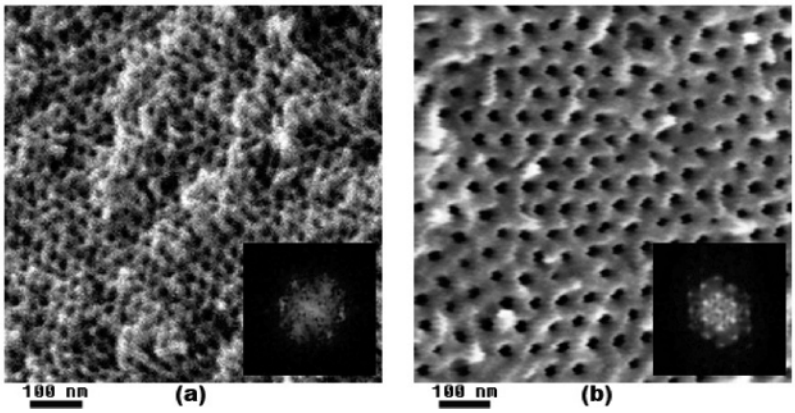

Figure 6. SEM pictures of (a) AS-3-HF and (b) DAS-1-HF. The inset in (a) shows a Fourier transform of a 330 nm × 330 nm region in the SEM picture of AS-3-HF, and the inset in (b) shows a Fourier transform of a 550 nm × 550 nm region in the SEM picture of DAS-1-HF.

spacer between the lamellar polymeric sheets, and the individual sheets of polystyrene can skew up a little and not be perfectly parallel, as illustrated in Figure 5. For this reason the scattering peaks of AS-1-HF are expected to show a broad distribution of lamella spacing with the collapsed lamellae spacing as the lower boundary(marked by filled symbol in Figure 4a), i.e., lamellae without real cavity in between, where the PAA chains from adjacent sheets overlap. Detailed information on electron density profiles that could be used to substantiate or reject such a possibility are currently missing. The position and width of the primary peaks were obtained by Lorentzian fit of each scattering profile.

The reason for the observed shrinkage of AS-1-HF could be related to the negative pressure generated by the urge of surface energy minimization and by the hydrogen bonds among the formed carboxylic acid groups. In the presence of water the major part of the shrinkage disappeared, as will be shown in the paragraph on water uptake.

A closer look at the SAXS profile in Figure 4 reveals that broadening of the primary peak also occurs in the case of the AS-3-HF sample but not at all in the case of DAS-1-HF. Both samples show hexagonal morphology, but the nanocavities are expected to be different. Assuming unaltered PS matrix the observed peak broadening indicates that the Bragg scattering planes are less well-defined in AS-3-HF than in its precursor AS-3. This could be due to heterogeneous cavity size and cavity filling by PAA in the etched sample, a combined effect of dispersities in polymer mass/composition and most importantly PAA conformational freezing. The last effect stands for the irreversible PAA structure freezing in the glassy state during sample drying (the glass transition temperature of bulk PAA is around 100 °C). The nanoporous sample cannot be annealed without deleting nanoporosity; therefore, the effect of PAA conformational freezing is difficult to erase in the dry state. However, in the presence of water filling the cavities the PAA chains become dynamically flexible and the freezing effect disappears. In the case of the triblock copolymer, PDMS is totally removed, and this leaves an empty volume in the center of the cylinders, with the consequence that the presence of cavities is less sensitive to the PAA conformational freezing and the Bragg planes are well-defined also in the nanoporous sample. This interpretation is supported by electron microscopy of the dry samples and SAXS in the presence of water (see the discussion relative to Figures 6 and 7).

SEM micrographs of AS-3-HF and DAS-1-HF are shown on the same scale of magnification in Figure 6. The fractured surface investigated in AS-3-HF was very rough as can be seen

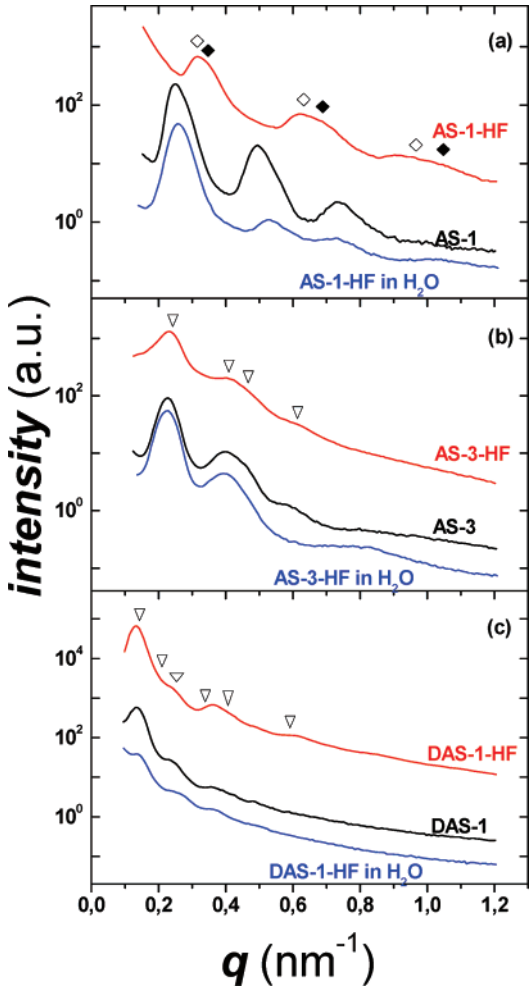

Figure 7. SAXS 1D profiles of (a) AS-1, AS-1-HF and AS-1-HF in H_2O (b) AS-3, AS-3-HF and AS-3-HF in H_2O and (c) DAS-1, DAS-1-HF and DAS-1-HF in H_2O. The scattering from the wet samples is observed at saturation water uptake.

in Figure 6a, which is due to increased sample brittleness correlating with the low molecular weight of the matrix polymer, PS. Both samples show hexagonal patterns of pores, with the distinct difference that the cavities for DAS-1-HF are larger and wider spread apart compared to the cavities for AS-1-HF. This is as expected from the molecular weights of the two samples and from the fact that the triblock sample sacrifices a larger portion of the molecule during degradation. The domain spacing (27 ± 3 and 46 ± 2 nm for AS-3-HF and DAS-1-HF, respectively) and pore radii (6 ± 1 and 11 ± 2 nm for the same

Table 2. Characterization Data of HF-Treated and TFA-Treated Samples in the Dry State and in the Presence of Water

	expected cavity volume[a] (vol %) dry								
sample	$\rho_{PAA} = 1.22$	$\rho_{PAA} = 1.00$	d_{SAXS}[b] (nm) dry	d_{SEM}[c] (nm) dry	r_{SAXS}[d] (nm) dry	r_{SEM}[e] (nm) dry	d_{SAXS}[f] (nm) wet	expected water uptake[g] (vol %)	obsd water uptake (vol %)
AS-1-HF	12	5.4	20	no[h]	1[i]		24	21	21
AS-3-HF	17	14	27	27 ± 3	6.1	6 ± 1	27	14	13
DAS-1-HF	27	25	47	46 ± 2	14	11 ± 2	47	25	24
DAS-1-TFA	27	25	47		14		47	25	24

[a] Based on SAXS results of the dry etched samples and block composition. The density values used to calculate the cavity volume were $\rho_{PS} = 1.05$ g/cm^3,[39] $\rho_{PtBA} = 1.00$ g/cm^3,[40] $\rho_{PAA} = 1.22$ g/cm^3,[39] (left), and $\rho_{PAA} = 1.00$ g/cm^3 (right); see text; $\rho_{PDMS} = 0.966$ g/cm^3.[39,41] [b] Principal spacings d_{10} or lamellar spacing period d from SAXS. [c] Principal d_{10} spacings from SEM. [d] Pore radii calculated as shown in the text from d_{SAXS} and composition, assuming $\rho_{PAA} = 1.00$ g/cm^3. [e] Pore radius from SEM. [g] Based on d_{SAXS} and block compostion. The density of PAA block plus water is arbitrarily taken 1.00 g/cm^3. [h] It was not possible to recognize any structure by SEM. [i] Expected lamellar cavity height, d_{cavity}.

samples, respectively) estimated from the SEM pictures were in good agreement with those obtained from the SAXS analysis (domain spacing, 27 and 47 nm, and pore radii, 6 and 14 nm, for the same samples, respectively), as listed in Table 2. Some of the pores in Figure 6 are visibly blocked or show lower contrast relative to the matrix. This feature is more pronounced in the case of sample AS-3-HF (Figure 6a). The significant surface roughness of this sample hinders a clear analysis. The fast Fourier transform (FFT) of Figure 6a hints to less well-defined Bragg planes than in the case of Figure 6b. This is in accordance with the SAXS profile of Figure 4b showing broadening of the structural peaks in the case of the AS-3-HF sample. Freeze fracture samples were prepared from AS-1-HF, but no successful micrographs were recorded. Both the lamellar morphology and the quite low molecular weight of PS concur to produce high sample brittleness.

The deprotection reaction removes 44% of the P*t*BA polymer mass transforming it into PAA. The contour length and the number of chains are expected to be conserved in the process, but the way the PAA chains pack and their mass density in the nanoporous polymers are unknown. Expected cavity volume fractions after degradation are listed in the second and third columns of Table 2. Two values were calculated on the basis of SAXS data for the etched samples and the copolymer composition values. The first was calculated under the assumption that the generated PAA has the same density as PAA's bulk density reported in the literature and the second under the rather arbitrary assumption of PAA density equal to 1 g/cm^3. Qualitatively, this last assumption followed by the appreciation that the PAA chain density in the interface with PS is the same as the chain density of the bulkier P*t*BA precursor; therefore, the density of PAA in the etched samples is expected to be lower than the bulk density of PAA. In the next section on water uptake it will be seen that the pore volumes calculated with the lower density value of PAA are in satisfactory agreement with the observed volumes of absorbed water. Columns 4−7 in Table 2 list the characteristic length scale for the etched samples in the dry state as investigated by SAXS and SEM.

Assuming identical matrix structure before and after acid treatment, the pore radii of AS-3-HF, DAS-1-HF, and DAS-1-TFA from the SAXS profiles were calculated to 6, 14, and 14 nm (see column 6 in Table 2) by using the following relation:

$$r_{SAXS} = d_{SAXS}\sqrt{\frac{2}{\pi\sqrt{3}}(1 - f_{PS} - f_{PAA})}$$

f_{PS} and f_{PAA} are volume fraction of PS and PAA block, respectively, and d_{SAXS} is the principal domain d_{10} spacing. The assumption of unchanged matrix is reasonable for the three samples with HEX structure, given the constancy of the respective scattering vectors before and after the acid treatments. Obviously, this assumption is not true for sample AS-1-HF. The concept of matrix is meaningless in this case. An average cavity height d_{cavity} of roughly 1 nm (see first entry in column 6) could be calculated for this sample by

$$d_{cavity} = d_{SAXS(AS-1-HF)} - d_{SAXS(AS-1)}(f_{PS} + f_{PAA})$$

on the basis of the SAXS lamella periods for the etched sample (first entry in column 4 of Table 2) and for the block copolymer precursor (first entry in the last column of Table 1), combined with volume composition data. The volume fraction f_{PAA} in the above relations was calculated assuming a PAA density of 1 g/cm^3.

Water Uptake. A direct proof of hydrophilicity for the nanoporous materials presented here was the spontaneous uptake of water. The four nanoporous PAA-*b*-PS samples—AS-1-HF, AS-3-HF, DAS-1-HF, and DAS-1-TFA—were placed into glass vials containing distilled water. For comparison, a gyroid nanoporous PS sample prepared from PS-*b*-PDMS diblock copolymer precursor[22] was also placed into a glass vial containing pure water. After soaking in water for 1 day, the four PAA-*b*-PS samples sank down to the bottom of their respective vials. Volumes of water uptake for AS-3-HF, DAS-1-HF, and DAS-1-TFA were close to the expected volumes (see the last two columns in Table 2). The gyroid nanoporous PS sample from PS-*b*-PDMS precursor floated on the surface of water and was not able to take any water within 3 weeks. This confirms that hydrophilic nanopores were created in the four PS-*b*-PAA samples.

The morphologies of the three nanoporous PAA-*b*-PS samples in water were investigated by SAXS, and Figure 7 shows the resulting data.

Compared to the dry state the position of the primary peak for AS-1-HF in water shifted back to a smaller q value (0.260 nm^{-1}) and the scattering peaks became narrower, indicating expansion in the lamellar structure during water uptake. The primary scattering peak in water is similar to that of the original AS-1 diblock copolymer, while the higher order reflections are reduced. This suggests that water penetrates the sample and fills up the space originally occupied by the *tert*-butyl groups, and the lamellar morphology of the PS matrix is restored, though with reduced long-range ordering.[42]

Within ±1%, the positions of primary peaks for AS-3-HF and DAS-1-HF do not change before and after water uptake. Soaking these samples in water produces to some degree reverse effects in the scattering profiles relative to the creation of nanoporosity by degradation. For example, the scattering from the samples AS-3-HF and DAS-1-HF in Figure 7 (panels b and c) show an overall drop in scattering intensity in the presence

of water due to a reduced scattering contrast. The SAXS profile of the wet sample AS-3-HF in H_2O is quite similar to the profile of the precursor AS-3. The principal peak is of similar width in the two cases. This indicates that the Bragg planes in the wet sample are better defined than in the dry AS-3-HF sample. At a PAA mass concentration of roughly 50%, as is the case with water filling the cavities, the glass transition temperature of PAA falls below room temperature, rendering the chains dynamically flexible; the electron density profiles in the different pores become more similar, and therefore the definition of the Bragg planes is reestablished.

The effect of reduced electron density (ρ_e) contrast is especially visible for the DAS-1-HF sample in water where the structural peaks are quite weak. Given the larger mass fraction of water in the cavities of this sample, the average ρ_e in the cavities can be estimated as that of water (0.556 mol/cm^3). This value is quite close to the ρ_e for PS (0.565 mol/cm^3). The electron density difference $\rho_{e,PS} - \rho_{e,H_2O}$ is 4−5 times lower in this case than the electron density difference between PS and PDMS ($\rho_{e,PDMS} = 0.522$ mol/cm^3) in the unetched sample. More refined considerations, which take into account the electron density contribution of PAA do not alter the conclusion of reduced contrast.

Conclusions

Nanoporous poly(acrylic acid)-*b*-polystyrene amphiphilic diblock copolymers with hydrophilic cavity surfaces were successfully prepared for the first time from P*t*BA-*b*-PS and PDMS-*b*-P*t*BA-*b*-PS copolymer precursors. The combination of living anionic polymerization and ATRP allows synthesizing PDMS-*b*-P*t*BA-*b*-PS triblock copolymer with a center P*t*BA block, which can be modified to the hydrophilic PAA and PDMS block that can be fully degraded. Deprotection of *tert*-butyl groups in P*t*BA and selective etching of PDMS chains were accomplished by applying HF or TFA in one step. Two different morphologies, lamellae and cylinders, have been achieved through the self-assembly of block copolymers as evidenced by SAXS. The hydrophilic property of nano cavity surfaces in the PAA-*b*-PS block copolymers was verified by water uptake measurements. The nanoporous polymers prepared in this work are expected to broaden the spectrum of possible applications of such materials in cases, which require aqueous or biological environment. In prospect, both the bulkiness of the protecting group in the acrylate polymer (*tert*-butyl in the present case) and the length of the PDMS chain can be used as controlling handles for the porosity and pore size.

Acknowledgment. This work was supported by the Danish Research Council for Technology and Production Sciences (FTP Grant 26-03-0271). We thank Rolf H. Berg at Risø for useful discussions. We thank Pia Wahlberg from Center for Microtechnology and Surface Analysis at the Danish Technological Institute for the SEM measurements.

Supporting Information Available: Experimental details. This material is available free of charge via the Internet at http://pubs.acs.org.

References and Notes

(1) Thurn-Albrecht, T.; Schotter, J.; Kastle, G. A.; Emley, N.; Shibauchi, T.; Krusin-Elbaum, L.; Guarini, K.; Black, C. T.; Tuominen, M. T.; Russell, T. P. *Science* **2000**, *290*, 2126.
(2) Hou, S.; Harrell, C. C.; Trofin, L.; Kohli, P.; Martin, C. R. *J. Am. Chem. Chem. Soc.* **2004**, *126*, 5674.
(3) Johnson, B. J. S.; Wolf, J. H.; Zalusky, A. S.; Hillmyer, M. A. *Chem. Mater.* **2004**, *16*, 2909.
(4) Kim, D. H.; Jia, X.; Lin, Z.; Guarini, K.; Russell, T. P. *Adv. Mater.* **2004**, *16*, 702.
(5) Sertova, N.; Toulemonde, M.; Hegmann, T. *J. Inorg. Organomet. Polym. Mater.* **2006**, *16*, 91.
(6) Yang, S. Y.; Ryu, I.; Kim, H. Y.; Kim, J. K.; Jang, S. K.; Russell, T. P. *Adv. Mater.* **2006**, *18*, 709.
(7) Yang, B.; Aksak, B.; Lin,Q.; Sitti, M. *Sens. Actuators B* **2006**, *114*, 254.
(8) Segalman, R. A.; Hexemer, A.; Kramer, E. J. *Macromolecules* **2003**, *36*, 6831.
(9) Zhang, Q.; Xu, T.; Butterfield, D.; Misner, M. J.; Ryu, D. Y.; Emrick, T.; Russell, T. P. *Nano Lett.* **2005**, *5*, 357.
(10) Germain, J.; Hradil, J.; Frechet, J. M. J.; Svec, F. *Chem. Mater.* **2006**, *18*, 4430.
(11) Hillmyer, M. A. *Adv. Polym. Sci.* **2005**, *190*, 137.
(12) Lee, J.-S.; Hirao, A.; Nakahama, S. *Macromolecules* **1988**, *21*, 274.
(13) Liu, G.; Ding, J.; Guo, A.; Herfort, M.; Bazett-Jones, D. *Macromolecules* **1997**, *30*, 1851.
(14) Liu, G.; Ding, J.; Stewart, S. *Angew. Chem., Int. Ed.* **1999**, *38*, 835.
(15) Mao, H.; Arrechea, P. L.; Bailey, T. S.; Johnson, B. J. S.; Hillmyer, M. A. *Faraday Discuss.* **2005**, *128*, 149.
(16) Rzayev, J.; Hillmyer, M. A. *Macromolecules* **2005**, *38*, 3.
(17) Matyjaszewski, K.; Xia, J. *Chem. Rev.* **2001**, *101*, 2921.
(18) Morton, B. M. *Anionic Polymerization: Principles and Practice*; Academic Press: New York, 1983.
(19) Hietala, S.; Mononen, P.; Strandman, S.; Jarvi, P.; Torkkeli, M.; Jankova, K.; Hvilsted, S.; Tenhu, H. *Polymer* **2007**, *48*, 4087.
(20) Ndoni, S.; Papadakis, C. M.; Almdal, K.; Bates, F. S. *Rev. Sci. Instrum.* **1995**, *66*, 1090.
(21) Merrifield, R. B. *J. Am. Chem. Soc.* **1963**, *85*, 2149.
(22) Ndoni, S.; Vigild, M. E.; Berg, R. H. *J. Am. Chem. Soc.* **2003**, *125*, 13366.
(23) Nakagawa, Y.; Miller, P. J.; Matyjaszewski, K. *Polymer* **1998**, *39*, 5163.
(24) Miller, P. J.; Matyjaszewski, K. *Macromolecules* **1999**, *32*, 8760.
(25) Kurjata, J.; Chojnowski, J.; Yeoh, C.-T.; Rossi, N. A. A.; Holder, S. J. *Polymer* **2004**, *45*, 6111.
(26) Rutnakornpituk, M.; Ngamdee, P.; Phinyocheep, P. *Polymer* **2005**, *46*, 9742.
(27) Jankova, K.; Chen, X.; Kops, J.; Batsberg, W. *Macromolecules* **1998**, *31*, 538.
(28) Guo, F.; Andreasen, J. W.; Vigild, M. E.; Ndoni, S. *Macromolecules* **2007**, *40*, 3669.
(29) Schulte, L.; Szewczykowski, P.P.; Guo, F.; Andersen, K.; Vigild, M. E.; Berg, R. H.; Ndoni, S. Submitted for publication.
(30) Hyman, H. H.; Garber, R. A. *J. Am. Chem. Soc.* **1959**, *81*, 1847.
(31) Willson, C. G.; Ito, H. *J. Electrochem. Soc.* **1986**, *133*, 181. See also: MacDonald, S. A.; Willson, C. G.; Fréchet, M. J. *Acc. Chem. Res.* **1994**, *27*, 151. Ichikawa, R.; Hata, M.; Okimoto, N.; Oikawa-Handa, S.; Tsuda, M. *J. Polym. Sci., Part A: Polym. Chem.* **1998**, *36*, 1035.
(32) Ma, Q.; Wooley, K. L. *J. Polym. Sci., Part A: Polym. Chem.* **2000**, *38*, 4805. See also: Clements, J. H.; Weber, S. E. *J. Phys. Chem. A* **1999**, *103*, 2513. The firs report found on the TFA/CH_2Cl_2 *t*-Bu ester deprotection in organic chemistry is from: Bryan, D. B.; Hall, R. F.; Holden, K. G.; Huffman, W. F.; Gleason, J. G. *J. Am. Chem. Soc.* **1977**, *99*, 2353.
(33) Davis, K. A.; Matyjaszewski, K. *Macromolecules* **2000**, *33*, 4039.
(34) Yang, D.; Li, L.; Wang, C. *Mater. Chem. Phys.* **2004**, *87*, 114.
(35) Wilczek, L.; Chojnowski, J. *Macromolecules* **1981**, *14*, 9.
(36) Sigwalt, P. *Polym. J.* **1987**, *19*, 567.
(37) DeSimone, J. M.; Paisner, S. N. US Patent Appl. Pub. 20030180522 A1, 2003. See also: Paisner, S. N.; DeSimone, J. M. *Abstracts of Papers*, 224th ACS National Meeting, Boston, MA, Aug 18−22, 2002.
(38) See the Supporting Information.
(39) Mark, J. E., Ed. *Polymer Data Handbook*; Oxford University Press: New York, 1999.
(40) van Krevelen, D. W.; Hoftyzer, P. J. *Properties of Polymers*; Elsevier: Amsterdam, 1976.
(41) Brandrup, J.; Immergut, E. H. *Polymer Handbook*, 3rd ed.; John Wiley & Sons: New York, 1989.
(42) A priori such a lamellar structure is not expected to show memory in the presence of water. Actually, we expect a well-aligned sample to disintegrate by exfoliation during acidolysis. This is indeed the case, as explained in the Supporting Information.[38] The fact that the sample described in this paper did not exfoliate is quite probably due to the missing of lamella alignment; some kind of topological interlocking of the lamellae would then be responsible for the observed sample stability. It cannot be excluded that morphological defects such as lamella ramifications also play a stabilizing role. On these grounds the observed curious structure reversing in the presence of water is considered coincidental.

MA0718806